Mixed Convective flow over a Stretching Surface with variable thermal conductivity and Binary Chemical reaction

S. ANURADHA[1] and M. PRIYA[2]

[1]Professor & Head in Department of Mathematics, Hindusthan College of Arts & Science, Coimbatore-641028, Tamilnadu, India. E-mail: researchhmt@gmail.com

[2]Research Scholar in Department of mathematics, Hindusthan College of Arts & Science, Coimbatore-641028, Tamilnadu, India, E-mail: priya.jeni28@gmail.com

[*]**Corresponding author: priya.jeni28@gmail.com**

Abstract: A coupled nonlinear boundary value problem arising from a mixed convective flow of a non-newtonian Casson fluid at a stretching surface with variable thermal conductivity and Binary chemical reaction is investigated in this paper. Using a similarity transformation, the governing equations are transformed into a system of coupled, nonlinear ordinary differential equations and the Numerical solutions for the velocity, temperature and concentration fields are obtained via a bvp4c MATLAB solver. The characteristics of the velocity, temperature and concentration fields in the boundary layer have been analyzed for several sets of values of the Hartman number, the Prandtl number, the Eckert number, the thermal and Mass Grashof number, the temperature relative parameter, Activation energy, Chemical reaction parameter and the Fitted rate constant. The presented results through graphs and tables reveal substantial effects of the pertinent parameters on the flow, heat and Mass transfer characteristics. The numerical consequences are in suitable settlement with those of results formerly published in the literature.

Keywords: Variable thermal conductivity, Mixed convective, Eckert number, Activation energy, Prandtl number, Grashof number, Chemical reaction.

1. INTRODUCTION

The study of heat and mass transfer acquired giant interest in many theoretical and experimental or practical aspects because of its various applications in industry, scientific, and engineering strategies. Mass transfer process with chemical reaction has been given special attention in the past because of its significance in chemical engineering, geothermal reservoirs, nuclear reactor cooling and thermal oil recovery. In the literature, such issues are dealt with the non-newtonian fluids via a stretching surface with different boundary conditions. Anuradha and Sasikala [1] obtained numerical solutions for two-dimensional MHD mixed convection flow with binary chemical reaction effect using Finite difference method. Ashraf et al., [2] explored mixed convection Casson fluid flow under the consideration of hall effect and convective boundary conditions. Atif et al., [3] put light on MHD Casson nanofluid under the influence of exponential temperature dependent thermal conductivity and Arrhenius activation energy past a stretching surface using Shooting technique. Das [4] examined MHD Mixed convective Casson fluid for the influence of viscous dissipation and thermal radiation over a porous inclined plate using MATLAB bvp4c method. Dessie and Fissha [5] utilized R-K Fourth order method to portray the impact of Mixed convective Maxwell nanofluid past a porous vertical sheet with chemical reaction. Dhlamini et al., [6] have explored the One -dimensional stream of viscous nanofluid flow in presence of Binary chemical reaction and Activation energy using Spectral quasi-linearization method (SQLM). The problem Mixed convection flow of MHD Williamson Nanofluid subject to Arrhenius Activation Energy was solved by Eswaramoorthi et al., [7]. Gangaiah et al., [8] illustrate the consequence of MHD flow of Casson nanofluid on an exponentially stretching sheet using Runge-Kutta fourth order along with Shooting technique. Gbadeyan et al., [9] used Galerkin weighted residual method (GWRM) to study the effect of variable thermal conductivity and viscosity on Casson nanofluid with velocity slip. Numerical study of MHD Mixed convection Jeffrey fluid flow over an extending sheet was analysed by Harish babu and Satya Narayana [10]. Ibrahim and Anbessa [11] computed three-dimensional Casson Nanofluid flow with Mixed convection, Hall and slip effects. Idowu et al., [12] numerically contemplated MHD dissipative Casson fluid flow with variable viscosity and thermal conductivity effects using Chebyshev collocation spectral approach. Ijaz et al., [13] considered an Activation energy mechanism in radiative flow of Sisko nanofluid. The homotopic approach is used to obtain the series solution of melting heat transfer in MHD flow with activation energy was established by Javed et al., [14]. Khan et al., [15] explained the behavior of activation energy with the binary reaction on MHD flow of titanium alloy (Ti6Al4V) nanoparticle along with a cross flow and streamwise direction using bvp4c MATLAB package. Kumar et al., [16] numerically examined flow and heat transfer of tangent hyperbolic fluid with Arrhenius activation energy using R-K45 numerical technique. Lu et al., [17] scrutinized the effect of Binary chemical reaction on three- dimensional rotating flow. Mahanta and Shaw [18]

numerically contemplated the Casson fluid flow with convective boundary condition using Spectral Relaxation Method. Majeed et al., [19] have investigated numerical analysis of MHD flow with Binary chemical reaction and second order momentum slip. Mondal et al., [20] inspected the flow movement of a Casson fluid under the consideration of Variable Viscosity and Thermal Conductivity Effects utilizing explicit finite differential technique. Mustafa et al., [21] numerically examined the results of Binary chemical reaction and activation energy on MHD nanofluid flow past a vertical surface under buoyancy effects. Nawaza et al., [22] conferred a model to describe the Magnetohydrodynamic axisymmetric flow of Casson fluid with variable thermal conductivity to provide the result. Ragupathi et al., [23] demonstrated the 3D flow in a Casson Nanofluid considering the Arrhenius Activation Energy and Exponential Heat Source effects at the boundary of the stretching sheet. Sivasankaran et al., [24] using Runge–Kutta–Fehlberg method along with shooting technique to examine the problem of MHD Mixed convection stagnation point flow with chemical reaction and thermal radiation. Sohail et al., [25] concentrated on Casson fluid with effects of variable heat conductance and thermal conductivity on bi-directional stretching surface utilizing Optimal Homotopy Analysis Method (OHAM). MHD three dimensional Nanofluid flow past a bidirectional stretched surface with influence of binary chemical reactions, activation energy, thermophoresis and Brownian motion was premeditated by Sultan et al. [26]. Tufail et al., [27] inspected Chemical reaction effects on MHD Mixed convective flow using Lie Group analysis method. Yesodha et al., [28] addressed a mathematical model to investigate heat and mass transfer of Chemically reacting fluids with activation energy using numerical technique. Yusuf et al., [29] have been reported MHD stagnation point flow with Arrhenius Activation Energy and Melting Heat transfer effects. Ganga et al., [30] found numerical treatment of three-dimensional MHD non-newtonian Casson liquid flow towards a stretching surface with variable thermal conductivity using Fourth order R-K integration scheme. Shehzad et al.,[31] analyzed heat and mass transfer three dimensional Casson fluid flow in a porous medium channel under the consideration of Heat Generation using Homotopy Analysis Method (HAM).

An attempt has not been made till now to study the behavior of chemically reacting fluids with activation energy, Mixed convection and variable thermal conductivity. The authors have carried out work in this field for the major cause that this current article is to account for the outcome of variable thermal conductivity and Heat generation/absorption of chemically reacting fluid flow produced by an extending surface. The flow of non-newtonian Casson fluid has been attracted for the purpose of its widespread application in geophysics and production processes. Activation energy impact on the concentration of the fluid has additionally been carried out. MATLAB bvp4c package deal has been used for solving the nonlinear differential equations. The effects of pertinent parameter on velocity, temperature and concentration distributions are shown in graphically.

2.MATHEMATICAL FORMULATION

Consider the existence of Binary chemical reaction and variable thermal conductivity to a steady, incompressible, non-linear, three-dimensional boundary layer flow of Casson fluid. A stretching level surface induces the flow which coincides with the plane $z \geq 0$. The constant magnetic field is applying normal to the fluid flow and the induced magnetic field assumed to be negligible. Considering u (x, y, z), v (x, y, z) and w (x, y, z) are velocity components, T and T_∞ are the temperature and ambient temperature C and C_∞ are the concentration and concentration far away the surface. The fluid velocities on the surface are given by $U=ax, V=by$ and w=0 along the xy-plane, where a and b are constants. Thus, with the above assumptions and under the standard boundary layer suppositions, the resulting equations are (Nawaz et al., [22] and Ganga et al., [30])

Continuity Equation

$$\frac{\partial u}{\partial x}+\frac{\partial v}{\partial y}+\frac{\partial w}{\partial z}=0 \tag{1}$$

Momentum Equation

$$u\frac{\partial u}{\partial x}+v\frac{\partial u}{\partial y}+w\frac{\partial u}{\partial z}=\upsilon\left(1+\frac{1}{\beta}\right)\frac{\partial^2 u}{\partial z^2}-\frac{\sigma^* B_0^2}{\rho}u-\frac{\upsilon}{K}u+g\beta_T\left(T-T_\infty\right)+g\beta_C\left(C-C_\infty\right) \tag{2}$$

$$u\frac{\partial v}{\partial x}+v\frac{\partial v}{\partial y}+w\frac{\partial v}{\partial z}=\upsilon\left(1+\frac{1}{\beta}\right)\frac{\partial^2 v}{\partial z^2}-\frac{\sigma^* B_0^2}{\rho}v-\frac{\upsilon}{K}v \tag{3}$$

Energy Equation

$$u\frac{\partial T}{\partial x}+v\frac{\partial T}{\partial y}+w\frac{\partial T}{\partial z}=\frac{1}{\rho c_p}\frac{\partial}{\partial z}\left(k^*(T)\frac{\partial T}{\partial z}\right)+\frac{\sigma B_0^2}{\rho c_p}\left(u^2+v^2\right)+\frac{Q}{\rho c_p}\left(T-T_\infty\right) \tag{4}$$

Concentration Equation

$$u\frac{\partial C}{\partial x}+v\frac{\partial C}{\partial y}+w\frac{\partial C}{\partial z}=D_B\frac{\partial^2 C}{\partial z^2}-k_r^2\left(\frac{T}{T_\infty}\right)^n Exp\left(\frac{-E_a}{kT_1}\right)\left(C-C_\infty\right) \tag{5}$$

where u, v, and w are the velocity components along the x, y, and z directions, respectively. $\upsilon=\frac{\mu_B}{\rho}$ is the kinematic viscosity coefficient, $\beta=\mu_B\sqrt{\frac{2\pi_p}{p_y}}$ is the Casson fluid parameter, ρ is the density of the fluid, σ^* is the electrical conductivity, T is the fluid temperature, T_∞ the ambient temperature, T_w is the fluid temperature of the wall, C_w, C_∞ are near and far away the fluid concentration. Q is the volumetric heat generation/absorption coefficient. Temperature dependent thermal conductivity is $k^*(T)=k_\infty\left(1+\varepsilon\theta\right)$.Where k_∞ is the fluid free stream conductivity and ε is a small parameter. The term $k_r^2\left(\frac{T}{T_\infty}\right)^n Exp\left(\frac{-E_a}{kT_1}\right)\left(C-C_\infty\right)$ is the Modified Arrhenius function, E_a is the Activation energy, $k^2{}_r$ is the Chemical reaction rate constant, k_1 = 8.61×10–5 eV/K is the Boltzmann constant, n is a unitless constant exponent fitted rate constants typically lie in the range –1 < n < 1.

The conditions for boundary are

$$\left.\begin{aligned} &u=ax, v=by, \mathrm{w}=0, -k\frac{\partial T}{\partial z}=h_w\left(T_w-\mathrm{T}\right),\\ &C=C_w \end{aligned}\right\}\ at\ \ z=0$$
$$u=0,\quad v=0,\quad \mathrm{T}\to T_\infty,\quad C\to C_\infty \quad \text{as}\quad z\to\infty \tag{6}$$

3.METHOD OF SOLUTION

Utilizing the following variables

$$\eta=z\sqrt{\frac{a}{\upsilon}},u=axf'(\eta),v=ayg'(\eta)$$
$$\mathrm{w}=-\sqrt{a\upsilon}\left(f(\eta)+g(\eta)\right),\theta(\eta)=\frac{T-T_\infty}{T_w-T_\infty},\phi(\eta)=\frac{C-C_\infty}{C_w-C_\infty} \tag{7}$$

Continuity Eq. (1) is automatically satisfied. In view of Equation (7), Equations (2) – (6) become

$$\left(1+\frac{1}{\beta}\right)f'''+(f+g)f''-f'^2-\left(M^2+\frac{1}{\lambda}\right)f'+Gr\theta+Gc\phi=0 \tag{8}$$

$$\left(1+\frac{1}{\beta}\right)g'''+(f+g)g''-g'^2-\left(M^2+\frac{1}{\lambda}\right)g'=0 \tag{9}$$

$$(1+\varepsilon\theta)\theta''+\varepsilon\theta'^2+\Pr(f+g)\theta'+\Pr M^2 Ec\left(f'^2+g'^2\right)+\Pr B\theta=0 \tag{10}$$

$$\phi''+Sc\left[(f+g)\phi'-\sigma(1+\delta\theta)^n Exp\left(\frac{-E}{(1+\delta\theta)}\right)\phi\right]=0 \tag{11}$$

The relevant boundary conditions are

$$\begin{aligned} &f(0)=0, g(0)=0, f'(0)=1, g'(0)=\alpha, \theta(0)=1, \phi(0)=1 \text{ at } \eta=0 \\ &f'(\infty)\to 0, g'(\infty)\to 0, \theta(\infty)\to 0, \phi(\infty)\to 0 \quad \text{at } \eta\to\infty \end{aligned} \tag{12}$$

In the above equations the non-dimensional parameters M^2, λ, α, Gr_T, Gc_c, Ec, Pr, B, Sc, σ, δ, E, n stands for the Hartman number, Porosity parameter, Ratio parameter, Thermal Grashof number, Mass Grashof number, Eckert number, Prandtl number, Heat generation/absorption coefficient, Schmidt number, Chemical reaction parameter, Temperature relative parameter, Activation energy and Fitted rate constant respectively.

$$M^2=\frac{\sigma^* B_0^2}{a\rho} \quad \lambda=\frac{Ka}{\upsilon} \quad \alpha=\frac{b}{a} \quad Sc=\frac{\upsilon}{D_B} \quad \Pr=\frac{\upsilon}{\sigma} \quad B=\frac{Q}{a\rho c_p} \quad E=\frac{E_a}{k_1 T_\infty} \quad \delta=\frac{T_w-T_\infty}{T_\infty} \quad \sigma=\frac{k_r^2}{a}$$

$$Gr=\frac{g\beta_T(T_w-T_\infty)}{au} \quad Gc=\frac{g\beta_c(C_w-C_\infty)}{au}$$

Mathematical expression of skin friction coefficient is disclosed as follows:

$$C_{fx}=\frac{\tau_w x}{\rho u_w^2} \qquad C_{fy}=\frac{\tau_w y}{\rho u_w^2} \tag{13}$$

Non-dimensional mode is given as

$$\mathrm{Re}_x^{-\frac{1}{2}} C_{fx}=\left(1+\frac{1}{\beta}\right)f''(0) \tag{14}$$

$$\mathrm{Re}_y^{-\frac{1}{2}} C_{fy}=\left(1+\frac{1}{\beta}\right)g''(0) \tag{15}$$

Nusselt number for the present analysis is given as

$$Nu_x=-\frac{xq_w}{k(T_w-T_\infty)}$$

$$\mathrm{Re}_x^{-\frac{1}{2}} Nu_x=-\theta'(0) \tag{16}$$

Sherwood number for the present analysis is given as

$$Sh_x = -\frac{x j_w}{D(C_w - C_\infty)}$$

$$\mathrm{Re}_x^{-\frac{1}{2}} Sh_x = -\phi'(0) \tag{17}$$

Where $\mathrm{Re}_x = \frac{u_w x}{\upsilon}$ is definition of the Reynold's number.

4. METHODOLOGY

The ordinary differential equations (8) – (11) are coupled and highly non – linear and exact analytical solutions cannot be determined. Hence, these equations with the boundary conditions (12) are solved using bvp4c MATLAB package and obtained numerical solutions.

5. RESULTS AND DISCUSSION

The current section is devoted for the designated discussion approximately the physical behavior of the unknown physical quantities which include velocity profile $\left[f'(\eta), g'(\eta) \right]$, temperature distribution $\theta(\eta)$ and mass concentration $\phi(\eta)$ for numerous values of the regarded pertinent parameters in the flow model. The following pertinent parameters were used

$$\beta = 1.5, \lambda = 2.0, \alpha = 0.5, M = 0.6, \mathrm{Pr} = 0.9, B = 0.4, \varepsilon = 0.7$$
$$Gr = Gc = 1.0, n = 1, E = 1, \sigma = 0.3, \delta = 1, Sc = 0.6, Ec = 0.1$$

These values are kept constant throughout the study unless otherwise stated in the respective figures. The physical parameters involved in the flow model are the Hartman number (M^2), Thermal Grashof number (Gr), Mass Grashof number (Gc), Eckert number (Ec), Prandtl number (Pr), Chemical reaction parameter (σ), Temperature relative parameter (δ), Activation energy (E) and Fitted rate constant (n) for which the numerical results of considered properties are computed and demonstrated graphically in Figures.1-13.

5.1 Velocity profiles

Figures.1-4 sketches the impact of Thermal Grashof Number (Gr), Mass Grashof Number (Gc), Hartmann Number (M^2) and Prandtl number (Pr) on velocity graphs. Figures.1 and 2 explains that the fluid velocities are increases with higher values of Thermal and Mass Grashof number (Gr and Gc). The Gr indicates the relative effect of the thermal buoyancy force to the viscous hydromagnetic force in the boundary layer. Due to the enhancement of buoyancy effect both velocities are increased. The fluid velocities are having opposite behavior with the effects of Hartmann Number (M^2) and Prandtl number (Pr). From Figure.3 decrement in velocity field is noticed for enlarged values of Hartmann number. Also, momentum boundary layer thickness decays. It is because with enhanced Hatrmann number M^2 produces a large quantity of Lorentz force which is subjected to reduction of velocity. Figure.4 Fluids with lower Pr have higher thermal conductivity. So heat can defuse from the sheet faster than for higher Prandtl number fluids.

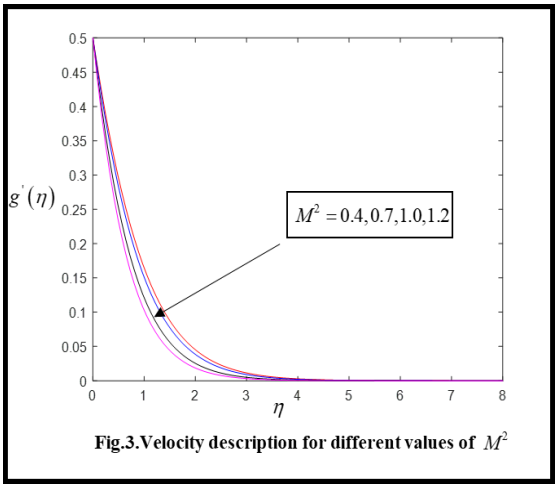

Fig.3.Velocity description for different values of M^2

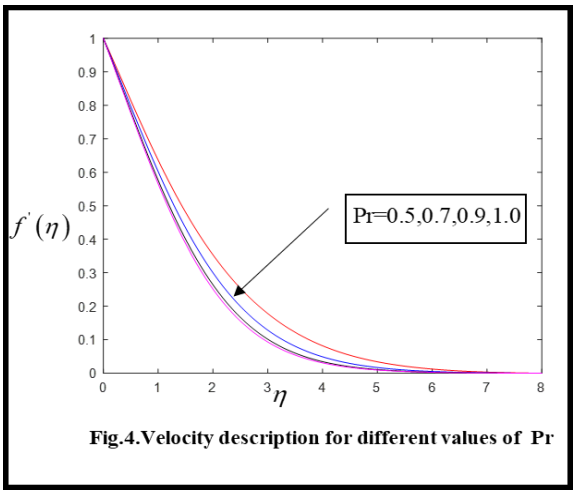

Fig.4.Velocity description for different values of Pr

5.2 Temperature profiles

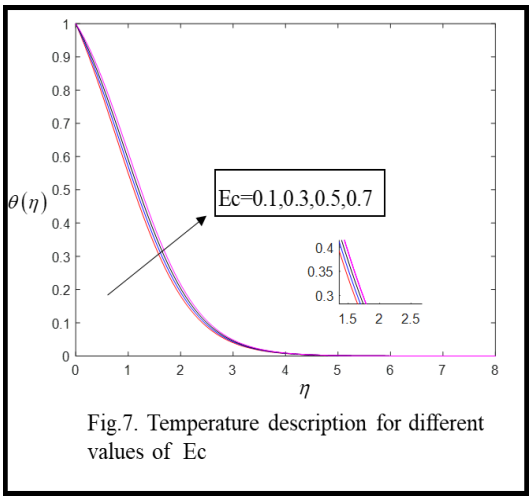

Fig.7. Temperature description for different values of Ec

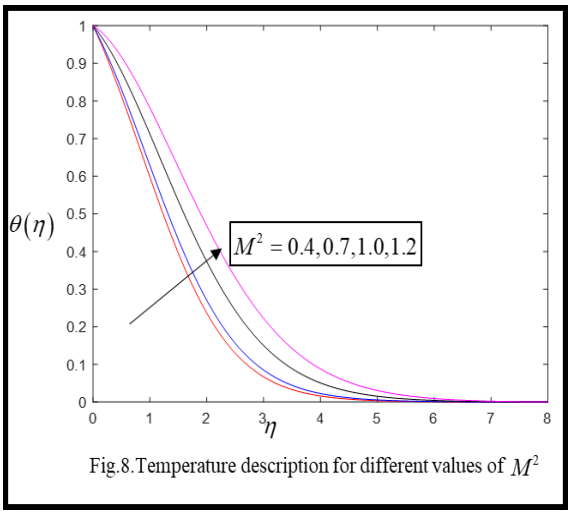

Fig.8.Temperature description for different values of M^2

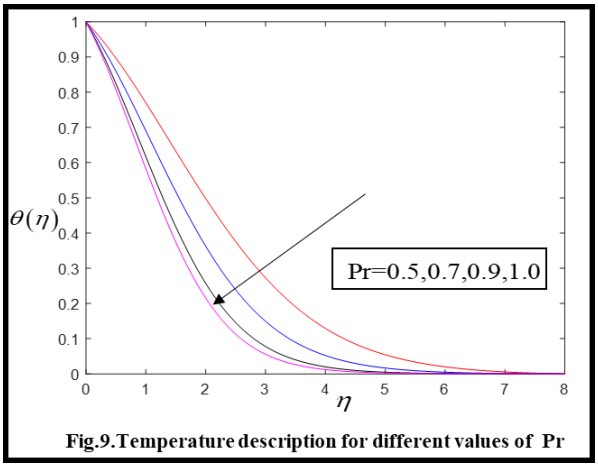

Fig.9.Temperature description for different values of Pr

Figures.5 - 9 demonstrate the variations of temperature profiles for distinctive values of Thermal Grashof Number (Gr), Mass Grashof Number (Gc), Eckert Number (Ec), Hartmann Number (M^2) and Prandtl number (Pr). Figures.5 and 6, Decrement in temperature field is observed for enlarged values of thermal and Mass Grashof number (Gr & Gc). Also, momentum boundary layer thickness decays. Figure.7 depicts the disparity of the temperature profile for various values of Eckert number (Ec). Higher values of Ec improve the thermal flow field. Due to the domination of viscosity in the flow we observed a mixed performance in the temperature field. It is exciting to mention that the influence of Ec is higher in the Casson fluid flow. The outcomes of Hartmann number on temperature field is displayed in Figure 8. Temperature profile grows clearly when Hartmann number M^2 grows. Thickness of thermal boundary layer also expands. The reason behind this is the manufacturing of Lorentz force. Maximum resistance produces because of Lorentz force due to which more heat will be generated and ultimately temperature profile raises. Figure.9 indicates that an augment in Prandtl Number (Pr) caused a decrease in temperature profiles. It can be seen that the temperature and thermal boundary layer thickness reduces with large values of Prandtl number (Pr).

5.3 Concentration profiles

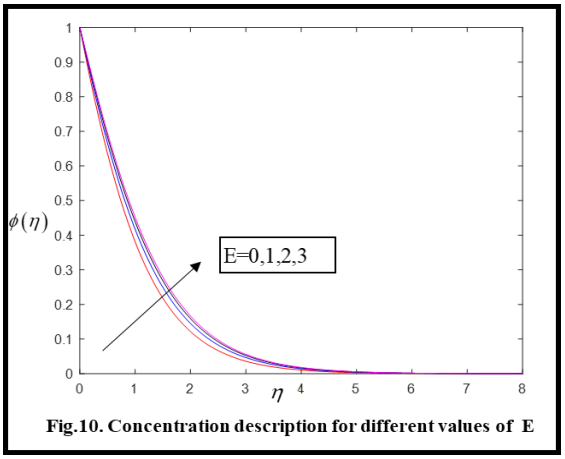

Fig.10. Concentration description for different values of E

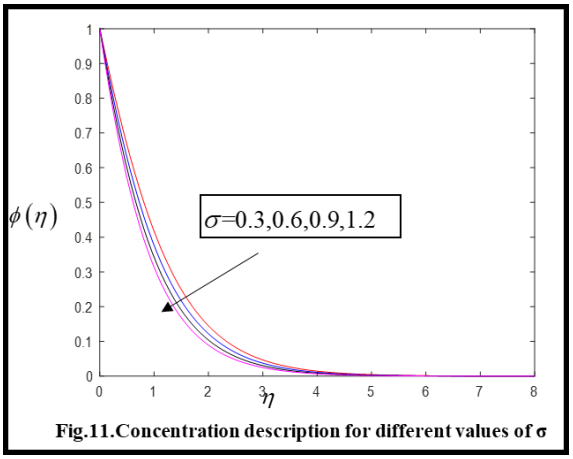

Fig.11.Concentration description for different values of σ

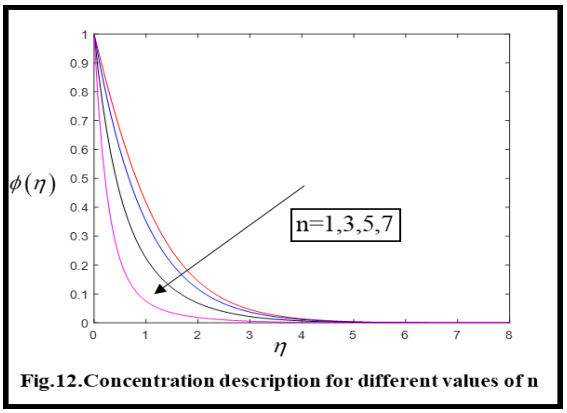

Fig.12.Concentration description for different values of n

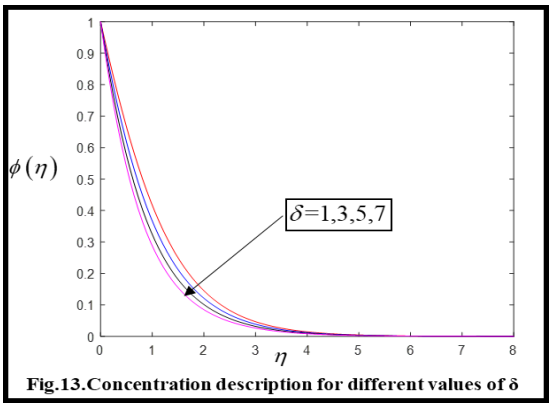

Fig.13.Concentration description for different values of δ

From Figures10–13 it is to learn the influence of a range of parameters like activation energy (E), Chemical reaction parameter (σ), fitted rate constant (n), and temperature relative parameter (δ) on concentration. Figure 10, we understand that when activation energy (E) enhances ϕ(η) thickness also increases. Enhanced activation energy results in destructive chemical reaction due to which concentration rises. In Figure 11, it is obvious that with raise in reaction rates σ values ϕ(η) come down rapidly. Figure 12 explain that ϕ(η) decreases for Fitted rate constant (n). When Fitted rate constant (n) amplifies, there is an increment in σ so automatically the liquid species terminate and reduces ϕ(η). Figure 13 reveals that elevating the values of δ leads to falling in ϕ(η). The factor $\sigma\left(1+\delta\theta\right)^{n}\exp\left(\frac{-E}{1+\delta\theta}\right)$ enhances for dominant δ. Therefore, concentration gradient enhances at the wall. Hence concentration profile diminishes.

Table 1. Comparison of Results for the Skin-Friction coefficient $f''(0), g''(0)$ for various values of α when $\beta \to \infty, \lambda \to \infty, M = 0$.

α	**Shehzed et al., [31]**		**Ganga et al., [30]**		**Present Results**	
	$-f''(0)$	$-g''(0)$	$-f''(0)$	$-g''(0)$	$-f''(0)$	$-g''(0)$
0	1	0	1	0	1.0000430	0
0.25	1.04881	1.19457	1.04881	0.19456	1.04871	1.19982
0.50	1.09309	0.46522	1.09309	0.46520	1.09343	0.47198
0.75	1.13450	0.79462	1.13448	0.79462	1.13448	0.79976
1.0	1.17372	1.17372	1.17372	1.17372	1.17295	1.17295

Conclusions

In this article we analyse the characteristics of chemical reaction of MHD Casson fluid with variable thermal conductivity and Mixed convection. The main outcomes of present study can be summarized as follows:

- The fluid velocities are increases with higher values of Thermal and Mass Grashof number (Gr and Gc).
- Hartman number M^2 has quite opposite effects on the velocities and temperature profiles. Thickness of thermal boundary layer also expands.
- Decrement in temperature field is observed for enlarged values of thermal and Mass Grashof number (Gr & Gc). Also, momentum boundary layer thickness decays. Higher values of Ec

improve the thermal flow field. It is exciting to mention that the influence of Ec is higher in the Casson fluid flow.

- An augment in Prandtl Number (Pr) caused a decrease in velocity and temperature profiles.
- An Activation energy (E) enhances $\phi(\eta)$ thickness also increases. Enhanced activation energy results in destructive chemical reaction due to which concentration rises.
- Raise in reaction rates σ values $\phi(\eta)$ come down rapidly. $\phi(\eta)$ decreases for Fitted rate constant (n).
- An Elevating value of δ leads to falling in $\phi(\eta)$. The factor $\sigma\left(1+\delta\theta\right)^{n}\exp\left(\frac{-E}{1+\delta\theta}\right)$ enhances for dominant δ. Therefore, concentration gradient enhances at the wall. Hence concentration profile diminishes.

It is hoped that the present study subsidized as a motivation for representing supplementary Mixed convective Magnetohydrodynamic Casson fluid flows with characteristics of chemical reactions are mainly in nuclear reactors, wind currents, heat exchangers and biomedicines. This article may be utilized in ground water hydrology, transpiration cooling, drilling activities, cell separation, car enterprise and solar energy harvesting and so on.

References

[1] Anuradha, S., and Sasikala, K., MHD Mixed Convection Stagnation Point Flow with Binary Chemical Reaction and Activation Energy, International Journal of Engineering and Techniques, 2017, Vol. 3, pp.320-325.

[2] Ashraf, M.B., Hayat, T., and Alsaedi, A., Mixed convection flow of Casson fluid over a stretching sheet with convective boundary conditions and Hall effect, Boundary Value Problems, 2017, Vol.137, pp.1-17, DOI 10.1186/s13661-017-0869-7.

[3] Atif, S.M., Shah, S., and Kamran, A., Effect of MHD on Casson fluid with Arrhenius activation energy and variable properties, Scientia Iranica, 2021, Vol.2021, pp.1-22, DOI:10.24200/SCI.2021.57873.5452.

[4] Das, U.J., MHD Mixed convective slip flow of Casson fluid over a porous inclined plate with joule heating, viscous dissipation and thermal radiation, J. math. comput. sci., 2021, Vol.11, pp. 3263-3275.

[5] Dessie, H., and Fissha, D., MHD Mixed Convective Flow of Maxwell Nanofluid Past a Porous Vertical Stretching Sheet in Presence of Chemical Reaction, Applications and Applied Mathematics: An International Journal (AAM), 2020, Vol. 15, pp. 530 – 549.

[6] Dhlamini, M., Kameswaran, P.K., Sibanda, P., Motsa, S., and Mondal, H., Activation energy and binary chemical reaction effects in mixed convective nanofluid flow with convective boundary conditions, Journal of Computational Design and Engineering,2019, Vol. 6, pp.149–158.

[7] Eswaramoorthi, S., Alessa, N., Sangeethavaanee, M., Kayikci, S., and Namgyel,N., Mixed Convection and Thermally Radiative Flow of MHD Williamson Nanofluid with Arrhenius Activation Energy and Cattaneo–Christov Heat-Mass Flux, Journal of Mathematics,Vol.2021, pp.1-16, https://doi.org/10.1155/2021/2490524.

[8] Gangaiah, T., Saidulu, N., and Venkata Lakshmi, A., The Influence of Thermal Radiation on Mixed Convection MHD Flow of a Casson Nanofluid over an Exponentially Stretching Sheet, Int. J. Nanosci. Nanotechnol., 2019, Vol. 15, pp. 83-98.

[9] Gbadeyan, J.A., Titiloye, E.O., and Adeosun, A.T., Effect of variable thermal conductivity and viscosity on Casson nanofluid flow with convective heating and velocity slip, Heliyon, 2020, Vol. 6, pp.1-10.

[10] Harish Babu, D., and Satya Narayana, P.V., Joule heating effects on MHD mixed convection of a Jeffrey fluid over a stretching sheet with power law heat flux: a numerical study, J. Magn. Magn. Mater., 2016, Vol.412, pp.185-193.

[11] Ibrahim, W., Anbessa, T., Three-Dimensional MHD Mixed Convection Flow of Casson Nanofluid with Hall and Ion Slip Effects, Mathematical Problems in Engineering Vol. 2020, Article ID 8656147, pp.1-15, https://doi.org/10.1155/2020/8656147.

[12] Idowu, A.S., Akolade, M.T., Abubakar, J.U., and Falodun, B.O., MHD free convective heat and mass transfer flow of dissipative Casson fluid with variable viscosity and thermal conductivity effects, Journal of Taibah University for Science, 2020, Vol.14, pp. 851– 862, https://doi.org/10.1080/16583655.2020.1781431.

[13] Ijaz, M., Ayub, M., Khan, H., Entropy generation and activation energy Mechanism in nonlinear radiative flow of Sisko nanofluid: rotating disk., Heliyon. 2019, Vol.5, pp.1-12.

[14] Javed, M., Alderremy, A. A., Farooq, M., Anjum, A., Ahmad, S., and Malik, M. Y., Analysis of activation energy and melting heat transfer in MHD flow with chemical reaction, European Physical Journal Plus, 2019, Vol. 134, pp.1-10.

[15] Khan, U., Zaib, A., Khan Ilyas., and Nisar, K.S., Activation energy on MHD flow of titanium alloy (Ti6Al4V) nanoparticle along with a cross flow and streamwise direction with binary chemical reaction and non-linear radiation: dual solutions., J. Mater. Res. Technol., 2020, Vol.9(1), pp.188-199.

[16] Kumar, K. G., Baslem, A., Prasannakumara, B. C., Majdoubi, J., Rahimi-Gorji, M., and Nadeem, S., Significance of Arrhenius activation energy in flow and heat transfer of tangent hyperbolic fluid with zero mass flux condition, Microsystem Technologies, 2020, Vol. 26, pp. 2517–2526.

[17] Lu, D.C., Ramzan, M., Bilal, M., Chung, J.D., and Farooq, U., A Numerical Investigation of 3D MHD Rotating Flow with Binary Chemical Reaction, Activation Energy and Non-Fourier Heat Flux, Commun. Theor. Phys., 2018, Vol.70, pp.89–96.

[18] Mahanta, G., and Shaw, S., 3D Casson fluid flow past a porous linearly stretching sheet with convective boundary condition, Alexandria Engineering Journal, 2015, Vol.54, pp. 653–659.

[19] Majeed A, Noori FM, Zeeshan A, Mahmood T, Rehman SU, Khan I., Analysis of activation energy in magnetohydrodynamic flow with chemical reaction and second order momentum slip model, Case Stud. Therm. Eng.,2018, Vol.12, pp.765-773.

[20] Mondal, R.K., Rabbi, S.R., Gharami, P.P., Ahmmed, S.F., and Arifuzzaman, S.M., A Simulation of Casson Fluid Flow with Variable Viscosity and Thermal Conductivity Effects, Mathematical Modelling of Engineering Problems,2019, Vol. 6, pp. 625-633.

[21] Mustafa, M., Khan, J. A., Hayat, T., and Alsaedi, A., Buoyancy effects on the MHD nanofluid flow past a vertical surface with chemical reaction and activation energy, International Journal of Heat and Mass Transfer, 2017, Vol. 108, pp. 1340–1346.

[22] Nawaza, M., Rahila Naza and Awaisb, M., Magnetohydrodynamic axisymmetric flow of Casson fluid with variable thermal conductivity and free stream, Alexandria Engineering Journal, 2018, Vol.57, pp.2043-2050, https://doi.org/10.1016/j.aej.2017.05.016.

[23] Ragupathi, P., Saranya, S., Mittal, H.V.R., and Al-Mdallal, Q.M., Computational Study on Three-Dimensional Convective Casson Nanofluid Flow past a Stretching Sheet with Arrhenius Activation Energy and Exponential Heat Source Effects, Modern Applications of Bioconvection with Fractional Derivatives, 2021, Vol.2021, pp.1-15, https://doi.org/10.1155/2021/5058751.

[24] Sivasankaran S, Niranjan H, Bhuvaneswari M., Chemical reaction, radiation and slip effects on MHD mixed convection stagnation-point flow in a porous medium with convective boundary condition, International Journal of Numerical Methods for Heat & Fluid Flow. 2017, Vol.27(2), pp.454–470.

[25] Sohail, M., Shah, Z., Tassaddiq, A., Kumam, P., and Roy, P., Entropy generation in MHD Casson fluid flow with variable heat conductance and thermal conductivity over non-linear bi-directional stretching surface, Scientific Reports, 2020, Vol.10, pp.1-16, https://doi.org/10.1038/s41598-020-69411-2.

[26] Sultan F, Khan WA, Ali M, Shahzad M, Irfan M, Khan M., Theoretical aspects of thermophoresis and Brownian motion for three-dimensional flow of the cross fluid with activation energy, Pramana. 2019, Vol.92, pp.1-10.

[27] Tufail M, N., Saleem, M., Chaudhry Q.A., Chemically reacting Mixed convective Casson fluid flow in the presence of MHD and porous medium through group theoretical analysis, Heat Transfer., 2020, Vol.49, pp.4657-4677, https://doi.org/10.1002/htj.21846.

[28] Yesodha, P., Bhuvaneswari, M., Sivasankaran, S., and Saravanan, K., Convective heat and mass transfer of Chemically reacting fluids with activation energy, radiation and heat generation, 2021, J.Ther .Eng., Vol. 7, No. 5, pp. 1130–1138.

[29] Yusuf, T.A., Wasiu, A., Salawu, S.O., and Gbadeyan, J.A., Arrhenius Activation Energy Effect on a Stagnation Point Slippery MHD Casson Nanofluid Flow with Entropy Generation and Melting Heat Transfer, Defect and Diffusion Forum, Vol.408, pp.1-18, DOI: https://doi.org/10.4028/www.scientific.net/DDF.408.1.

[30] Ganga, B., Charles, S., Abdul Hakeem, A.K., and Nadeem, S., Three dimensional MHD Casson fluid flow over a stretching surface with variable thermal conductivity, 2021, J.Appl.Math.Comp.Mech., Vol.20, pp.25-36.

[31] Shehzad, S.A., Hayat, T., and Alsaedi, A., Three-Dimensional MHD Flow of Casson Fluid in Porous Medium with Heat Generation, Journal of Applied Fluid Mechanics, 2016, Vol. 9, pp. 215-223.